
THE PREDICTIVE FORWARD-FORWARD ALGORITHM

Alexander Ororbia

Rochester Institute of Technology
ago@cs.rit.edu

Ankur Mali

University of South Florida
ankurarjunmali@usf.edu

ABSTRACT

In this work, we propose a generalization of the forward-forward (FF) algorithm that we call the predictive forward-forward (PFF) algorithm. Specifically, we design a dynamic, recurrent neural system that learns a directed generative circuit jointly and simultaneously with a representation circuit, combining elements of predictive coding, an emerging and viable neurobiological process theory of cortical function, with the forward-forward adaptation scheme. Furthermore, PFF efficiently learns to propagate learning signals and updates synapses with forward passes only, eliminating some of the key structural and computational constraints imposed by a backprop-based scheme. Besides computational advantages, the PFF process could be further useful for understanding the learning mechanisms behind biological neurons that make use of local (and global) signals despite missing feedback connections [11]. We run several experiments on image data and demonstrate that the PFF procedure works as well as backprop, offering a promising brain-inspired algorithm for classifying, reconstructing, and synthesizing data patterns. As a result, our approach presents further evidence of the promise afforded by backprop-alternative credit assignment algorithms within the context of brain-inspired computing.

Keywords Brain-inspired computing · Self-supervised learning · Neuromorphic · Forward learning

1 Introduction

The algorithm known as backpropagation of errors [38], or “backprop” for short, has long faced criticism concerning its neurobiological plausibility [8, 27, 12]. Despite having powered the tremendous progress and success behind deep learning and its every-growing myriad of promising applications [44, 9], it is improbable that backprop is a good, viable model of learning in the brain, such as in cortical regions. Notably, there are both practical and biophysical issues [12, 27], and among these issues are the following:

- there is a lack of evidence that neural activities are explicitly stored to be used later for synaptic adjustment,
- error derivatives are backpropagated along a global feedback pathway to generate teaching signals,
- the error signals move back along the same neural pathways used to forward propagate information, and,
- inference and learning are locked to be largely sequential (instead of massively/easily parallel).

Furthermore, in processing temporal data, it is certainly not the case that the neural circuitry of the brain is unfolded backwards through time in order to calculate and adjust synapses [33] (as it is for backprop through time).

Recently, there has been a growing interest in the research domain of brain-inspired computing, which focuses on developing algorithms and computational models that attempt to circumvent or resolve the critical issues such as those highlighted above. Among the most powerful and promising ones is predictive coding (PC) [15, 37, 10, 3, 40, 32], and among the most recent ones is the forward-forward (FF) algorithm [16]. These alternatives offer powerful, different means of conducting credit assignments that have shown similar performance as backprop, but to the contrary, are more likely consistent with and similar to real biological neuron learning (see Figure 1 for some representative credit assignment depictions). This paper will propose a novel model and learning/inference process, the **predictive forward-forward (PFF)** process, that generalizes and combines FF and PC into a robust (stochastic) neural system that simultaneously learns a representation and generative model in a biologically-plausible fashion. Like the FF algorithm, the PFF procedure offers a promising, potentially helpful model of biological neural circuits, a potential candidate system for low-power analog hardware and neuromorphic circuits, and a potential backprop-alternative worthy of future investigation and study.

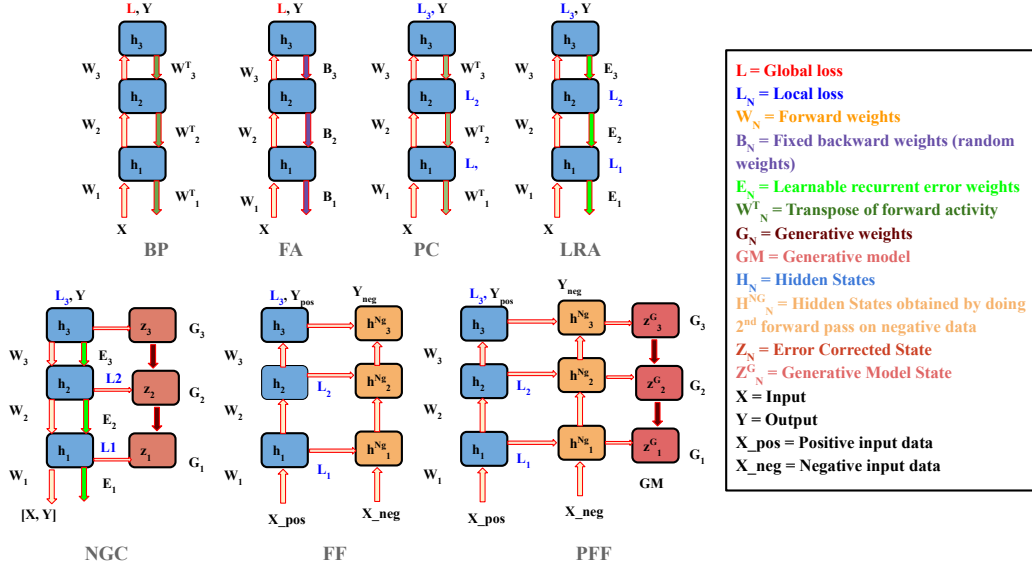


Figure 1: Comparison of learning algorithms that relax constraints imposed by backpropagation of errors (BP). Algorithms visually depicted include feedback alignment (FA) [26], predictive coding (PC) [37, 41], local representation alignment (LRA) [35], neural generative coding (NGC) [34, 32], the forward-forward procedure (FF) [16], and predictive forward-forward algorithm (PFF).

2 The Predictive Forward-Forward Learning Process

The brain-inspired neural process that we will design and study is called the predictive forward-forward (PFF) algorithm, which builds on and generalizes aspects of the FF algorithm [16]. At a high level, the PFF process consists of two neural structures or circuits, i.e., a representation circuit (parameterized by Θ_r) that focuses on acquiring distributed representations of data samples and a top-down generative circuit (parameterized by Θ_g) that focuses on learning to synthesize data given the activity values of the representation circuit. Thus, the PFF process can be characterized as a complementary system with the aim of jointly learning a classifier and generative model. We will first define the notation used throughout this paper, then proceed to describe the inference and learning mechanics of the representation circuit followed by those of the generative circuit.

Notation: We use \odot to indicate a Hadamard product and \cdot to denote a matrix/vector multiplication. $(\mathbf{v})^T$ is the transpose of \mathbf{v} . Matrices/vectors are depicted in bold font, e.g., matrix \mathbf{M} or vector \mathbf{v} (scalars shown in *italic*). \mathbf{z}_j will refer to extracting j th scalar from vector \mathbf{z} . Finally, $\|\mathbf{v}\|_2$ denotes the Euclidean norm of vector \mathbf{v} . The sensory input has shape $\mathbf{x} \in \mathcal{R}^{J_0 \times 1}$ (J_0 is the number of input features, e.g., pixels), label has shape $\mathbf{y} \in \mathcal{R}^{C \times 1}$ (where C is the number of classes), and any neural layer has shape $\mathbf{z}^\ell \in \mathcal{R}^{J_\ell \times 1}$ (J_ℓ is the number of neurons in layer ℓ).

2.1 The Forward-Forward Learning Rule

The PFF process, like the FF algorithm when it is applied to a recurrent network, involves adjusting the synaptic efficacies of a group of neurons by measuring their “goodness”, or, in other words, the probability that their activity indicates that an incoming signal comes from the target training data distribution (or the “positive class”). Formally, for any single layer ℓ in an L -layered neural system, we calculate the goodness as the sum of the squared activities for a given neural activity vector \mathbf{z}^ℓ and compare it to particular threshold value θ_z in one of two ways:

$$p(c=1)_\ell = \frac{1}{1 + \exp(-(\sum_j^{J_\ell} (\mathbf{z}_j^\ell)^2 - \theta_z))}, \text{ or, } p(c=1)_\ell = \frac{1}{1 + \exp(-(\theta_z - \sum_j^{J_\ell} (\mathbf{z}_j^\ell)^2))} \quad (1)$$

where $p(c=1)_\ell$ indicates the probability that the data comes from the data distribution (i.e., positive data, where the positive class is labeled $c=1$) while the probability that the data does not come from the training data distribution is $p(c=0)_\ell = 1 - p(c=1)_\ell$. Note that $p(c)_\ell$ indicates the probability that is assigned by a layer ℓ of neurons in a system/network. This means the cost function that any layer is trying to solve/optimize is akin to a binary class logistic regression problem formulated as follows:

$$\mathcal{L}(\Theta^\ell) = -\frac{1}{N} \sum_{i=1}^N c_i \log p(c_i=1)_\ell + (1 - c_i) \log p(c_i=0)_\ell \quad (2)$$

where the binary label c_i (the label for the i th datapoint \mathbf{x}_i) can be generated correctly and automatically if one formulates a generative process for producing negative data samples. Data patterns sampled from the training set $\mathbf{x}_j \sim \mathcal{D}_{train}$ can be labeled as $c_j = 1$ and patterns sampled outside of \mathcal{D}_{train} (from the negative data generating process) can be automatically labeled as $c_j = 0$. Crucial to the success of the FF procedure is the design of a useful negative data distribution, much as is the case for noise contrastive estimation [13].

It is important to notice that the FF learning rule is local in nature – this means that the synapses of any particular layer of neurons can be adjusted independently of the others. The rule’s form is furthermore different from a classical Hebbian update [14] (which produces a weight change by a product of incoming and outgoing neural activities), given that this synaptic adjustment requires knowledge across a group of neurons (goodness depends on the sum of squares of the activities of a group rather than an individual unit) and integrates contrastive learning into the dynamics. Synaptic updates are specifically calculated by taking the gradient of Equation 2, i.e., $\frac{\partial \mathcal{L}(\Theta^\ell)}{\partial \Theta^\ell}$. In effect, a neural layer optimizes Equation 2 by either maximizing the squared activities of a layer (to be above threshold θ_z) (left form of the probability presented in Equation 1) or, alternatively, minimizing the squared activities (right form of the probability presented in Equation 1).

2.2 The Representation Circuit

In order to take advantage of the above FF learning rule (and to model contextual prediction via top-down and bottom-up influences), a recurrent network was proposed in [16], where, at each layer, a set of top-down and bottom-up forces are combined to compute the activity of any layer ℓ , much akin to the inference process of a deep Boltzmann machine [39]. The core parameters of this model are housed in the construct $\Theta_r = \{\mathbf{W}^1, \mathbf{W}^2, \dots, \mathbf{W}^L\}$ (later referred to as the representation parameters). Note that no additional classification-specific parameters are included in our model (in contrast to the model of [16]), although incorporating these is straightforward.¹ Note that the representation circuit of the the PFF process will take the form of a recurrent network.

To compute any layer’s activity within the representation circuit, top-down and bottom-up messages are combined with an interpolation of the layer’s activity at the previous time step. Specifically, in PFF, this is done as follows:

$$\mathbf{z}^\ell(t) = \beta \left(\phi^\ell(\mathbf{W}^\ell \cdot \text{LN}(\mathbf{z}^{\ell-1}(t-1))) + \mathbf{V}^\ell \cdot \text{LN}(\mathbf{z}^{\ell+1}(t-1)) \right) + \epsilon_r^\ell + (1 - \beta)\mathbf{z}^\ell(t-1) \quad (3)$$

where $\epsilon_r^\ell \sim \mathcal{N}(0, \sigma)$ is injected, centered Gaussian noise and $\mathbf{z}^0(t-1) = \mathbf{x}$. As in [16], we set the activation function $\phi^\ell()$ for each layer ℓ to be the linear rectifier, i.e., $\phi^\ell(\mathbf{v}) = \max(0, \mathbf{v})$. Notice the introduction of an interpolation coefficient β , which allows integration of the state \mathbf{z}^ℓ over time (the new activity state at time t is a convex combination of the newly proposed state and the previous value of the state at $t-1$). Furthermore, notice that this interpolation is similar to that of the “regression” factor introduced into the recirculation algorithm [19], a classical local learning algorithm that made use of carefully crafted autoencoders to generate the signals needed for computing synaptic adjustments. $\text{LN}(\mathbf{z})$ is a layer normalization function applied to the activity vector, i.e., $\text{LN}(\mathbf{z}^\ell) = \mathbf{z}^\ell / (\|\mathbf{z}^\ell\|_2 + \epsilon)$ (ϵ is a small numerical stability factor for preventing division by zero). Note that the topmost layer of the representation circuit is clamped to a context vector \mathbf{y} (which could be provided by another neural circuit or be set to be a data point’s label/target vector), i.e., $\mathbf{z}^{L+1} = \mathbf{y}^2$, while the bottom layer is clamped to sensory input, i.e., $\mathbf{z}^0(t) = \mathbf{x}(t)$ (where $\mathbf{x}(t)$ could be the frame of video or a repeated copy of a static image \mathbf{x}). Equation 3 depicts a synchronous update of all layer-wise activities, but, as noted in [16], the recurrent model could alternatively be implemented by cycling between even and odd-number layers, i.e., first updating all even-numbered layers given the activities of the odd-numbered layers followed by updating the values of the odd-numbered layers given the new values of the even layers, much like the generative stochastic networks of [5].

To create the negative data needed to train this system, we disregard the current class indicated by the label \mathbf{y} of the positive data \mathbf{x}^p and create an incorrect “negative label” \mathbf{y}^n by randomly (uniformly) sampling an incorrect class index, excluding the correct one.³ A final mini-batch of samples is dynamically created by concatenating positive and negative samples, i.e., $\mathbf{x} = \langle \mathbf{x}, \mathbf{x} \rangle$ and $\mathbf{y} = \langle \mathbf{y}, \mathbf{y}^n \rangle$ (notice that positive image pixels are reused

¹If classification-specific parameters are desired, one could include an additional set of synaptic weights $\Theta^d = \{\mathbf{W}, \mathbf{b}\}$ that take in as input the top-most (normalized) activity $\text{LN}(\mathbf{z}^L)$ of the recurrent representation circuit in order to make a rough prediction of the label distribution over \mathbf{y} , i.e. $p(y = i | \text{LN}(\mathbf{z}^L)) = \exp(\mathbf{W} \cdot \text{LN}(\mathbf{z}^L) + \mathbf{b})_i / (\sum_c \exp(\mathbf{W} \cdot \text{LN}(\mathbf{z}^L) + \mathbf{b})_c)$. This would make the recurrent model of this work much more similar to that of [16]. Softmax parameters \mathbf{W} and \mathbf{b} would then be adjusted by taking the relevant gradients of the objective $\mathcal{L}^y(\mathbf{W}, \mathbf{b}) = -\log p(y = i | \text{LN}(\mathbf{z}^L))$.

²It is important to scale the label/context vector by a factor of about 5, i.e., the topmost layer activity would be $\mathbf{z}^{L+1} = \mathbf{y} * 5$ (Geoffrey Hinton, personal communication, Dec 12, 2022).

³This deviates from how the negative label was made in [16], which chose an incorrect class index in proportion to the probabilities produced by a forward pass of the classification-specific parameters. This was not needed for the PFF algorithm.

and paired with the negative labels in order to create the negative samples). The PFF process then involves running the combined mini-batch through the neural system and calculating the relevant synaptic updates.

Equation 3 is typically run several times (8 to 10 times as in this study and [16]), similar to the stimulus processing window that is simulated for predictive coding systems [37, 32]. Each time Equation 3 is run, the (bottom-up and top-down) synapses for layer ℓ are adjusted according to the following local update:

$$\Delta \mathbf{W}^\ell = \left(2 \frac{\partial \mathcal{L}(\Theta^\ell)}{\partial \sum_j^{J_\ell} (\mathbf{z}_j^\ell)^2} \odot \mathbf{z}^\ell \right) \cdot (\text{LN}(\mathbf{z}^{\ell-1}))^T, \text{ and, } \Delta \mathbf{V}^\ell = \left(2 \frac{\partial \mathcal{L}(\Theta^\ell)}{\partial \sum_j^{J_\ell} (\mathbf{z}_j^\ell)^2} \odot \mathbf{z}^\ell \right) \cdot (\text{LN}(\mathbf{z}^{\ell+1}))^T \quad (4)$$

which can then be applied to the relevant parameters, i.e., \mathbf{W}^ℓ and \mathbf{V}^ℓ , via methods such as stochastic gradient descent (SGD) with momentum or Adam [22]. In principle, the neural layers of the representation circuit are globally optimizing the objective $\mathcal{L}(\Theta_r) = \sum_{\ell=1}^L \mathcal{L}(\Theta^\ell = \mathbf{W}^\ell)$ (the summation of local goodness functions).

On Classifying Sensory Patterns: One might observe that our representation circuit does not include discriminatory parameters that classify inputs directly. Nevertheless, given that the supervised target \mathbf{y} is used as context to mediate the top-most latent representations of the recurrent circuit above, the representation system should (positive data samples) acquire distributed representations that implicitly encode label information. To take advantage of the discriminative information encoded in PFF’s representations, as was also done in the FF algorithm, we may still classify by executing an inference process similar to that of early hybrid Boltzmann machine models [23, 36]. Specifically, to classify an input \mathbf{x} , we iterate over all possible (one-hot) values that \mathbf{y} could be, starting with the first class index. Specifically, for any chosen \mathbf{y} (such as the one-hot encoding of class index i), we run Equation 3 for the representation circuit for T steps and then record the goodness across the layers in the middle three iterations (from $T/2 - 1$ to $T/2 + 1$), i.e., $\mathcal{G}_{y=i} = \frac{1}{3} \sum_{T/2-1}^{T/2+1} \frac{1}{L} \sum_{\ell=1}^L \theta_z - \sum_j^{J_\ell} (\mathbf{z}_j^\ell)^2$. This goodness calculation is made for all class indices $y = 1, 2, \dots, C$, resulting in $\{\mathcal{G}_{y=1}, \mathcal{G}_{y=2}, \dots, \mathcal{G}_{y=C}\}$ over which the argmax is applied in order to obtain the index of the class with the highest average goodness value. Note that, as mentioned in [16], if classification-specific parameters are included in PFF’s representation circuit, then a single feedforward pass could be used to obtain initial class probabilities. Then the above search could instead be simplified by conducting it over only the top M highest probabilities (and thus avoid an expensive search over a massive number of classes). To estimate the label probability distribution under the representation circuit, as we do in this work, we run the goodness (logits) through the softmax, i.e., $p(y = i | \mathbf{x}) \sim \exp(\mathcal{G}_i) / (\sum_c \exp(\mathcal{G}_c))$.

2.3 The Generative Circuit

As mentioned before, the PFF algorithm incorporates the joint adaptation of a top-down directed generative model. This aspect of the PFF process is motivated by the generative nature of predictive processing (PP) models [37, 10], particularly those that focus on learning a top-down generative model as in the framework of neural generative coding [32]. Crucially, we remark that jointly learning (in a biologically-plausible fashion) a generative feedback system could favorably provide a means of inspecting the content of the representations acquired by an FF-centric process as well as provide a plausible, alternative means for (internally) synthesizing negative data.

The generative circuit, which is comprised of the set of synaptic parameters $\Theta_g = \{\mathbf{G}^0, \mathbf{G}^1, \dots, \mathbf{G}^L\}$, attempts to learn how to predict, at each layer, a local region of neural activity, which, as we will see by design, facilitates simple error Hebbian updates (much like those calculated in a PP system). Formally, the objective that this generative circuit will attempt to optimize (for a single data point) is:

$$\mathcal{L}(\Theta_g) = \sum_{\ell=0}^L \mathcal{L}_g^\ell(\mathbf{G}^\ell) = \sum_{\ell=0}^L \sum_{j=1}^{J_\ell} (\bar{\mathbf{z}}_j^\ell - \mathbf{z}_j^\ell(t))^2 \quad (5)$$

where $\mathbf{z}^0 = \mathbf{x}$ (the bottom layer target is clamped to the data point being processed). Each layer of the generative circuit conducts the following computation:

$$\bar{\mathbf{z}}^\ell = g^\ell(\mathbf{G}^\ell \cdot \text{LN}(\hat{\mathbf{z}}^{\ell+1})), \text{ where, } \hat{\mathbf{z}}^{\ell+1} = \phi^{\ell+1}(\mathbf{z}^{\ell+1}(t) + \epsilon_z^{\ell+1}) \text{ and, } \mathbf{e}^\ell = \bar{\mathbf{z}}^\ell - \mathbf{z}^\ell(t) \quad (6)$$

$$\bar{\mathbf{z}}^L = g^L(\mathbf{G}^L \cdot \text{LN}(\mathbf{z}_s)), \text{ where, } \mathbf{z}_s \leftarrow \mathbf{z}_s - \gamma \frac{\partial \mathcal{L}_g^L(\mathbf{G}^L)}{\partial \mathbf{z}_s} \quad // \text{ Topmost latent layer activity } \mathbf{z}_s \quad (7)$$

where $\epsilon_z^\ell \sim \mathcal{N}(0, \sigma_z)$ is controlled (additive) activity noise injected into layer ℓ (with a small scale, such as $\sigma_z = 0.025$). $g^\ell()$ is the elementwise activation function applied to any generative layer’s prediction and, in this work, we set the activation functions for layers $\ell \geq 1$ to be the linear rectifier while the bottom one is specifically set to be the clipped identity, i.e., $g^0(\mathbf{v}) = \text{HardClip}(\mathbf{v}, 0, 1)$. At each step of the inference process that in Section

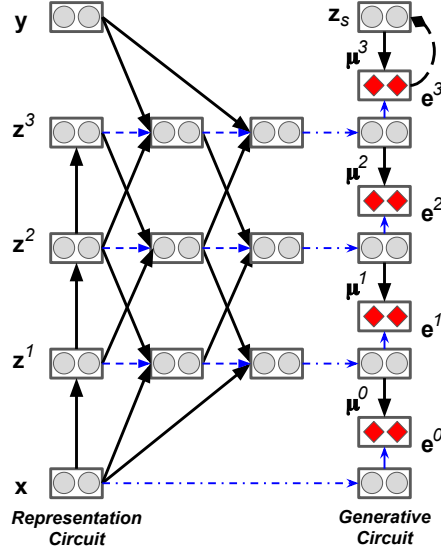


Figure 2: The PFF algorithmic process depicted over three-time steps for a three hidden layer network system coupled to a four-layer generative system (topmost layer is the sampled latent variable \mathbf{z}_s). Solid arrows represent synaptic weights, dashed blue arrows depict interpolation between left and right states, and dash-dotted arrows depict state carry-over/direct copying. The dashed diamond curve represents a feedback pathway, gray circles represent neural units, and red diamonds represent error neurons. Note that since all elements of the system are adjusted dynamically, the generative circuit is run/updated each time the representation circuit is run/updated.

2.2, the synaptic weights of the generative model (at each layer) are adjusted via the following Hebbian rule:

$$\Delta \mathbf{G}^\ell = \mathbf{e}^\ell \cdot (\text{LN}(\mathbf{z}^{\ell+1}(t)))^T, \text{ and } \Delta \mathbf{G}^L = \mathbf{e}^L \cdot (\text{LN}(\mathbf{z}_s))^T. \quad (8)$$

Notice that the topmost layer of the generative circuit (i.e., layer $L + 1$) is treated a bit differently from the rest, i.e., the highest latent generative layer \mathbf{z}_s predicts the topmost neural activity of the representation circuit \mathbf{z}^L and is then adjusted by an iterative inference feedback scheme, much akin to that of sparse/predictive coding [31, 37, 32]. Once trained, synthesizing data from the generative circuit can be done using ancestral sampling:

$$\bar{\mathbf{z}}^{L+1} = \mathbf{z}_s \sim P(\mathbf{z}_s) \quad (9)$$

$$\bar{\mathbf{z}}^\ell = g^\ell(\mathbf{G}^\ell \cdot \text{LN}(\bar{\mathbf{z}}^{\ell+1})), \ell = L, (L-1), \dots, 0 \quad (10)$$

where we choose the prior $P(\mathbf{z}_s)$ to be a Gaussian mixture model (GMM) with 10 components, which, in this study, was retro-fit to samples of the trained system's topmost activity values (acquired by running the training dataset \mathcal{D}_{train} through the model), as was done for the top-down directed generative PP models of [32]. Note that for all circuits in PFF (both the representation and generative circuits), we treat the derivative of the linear rectifier activation function as a vector of ones with the same shape as the layer activity \mathbf{z}^ℓ (as was done in [16]). The learning process of the PFF procedure is shown in Algorithm 1 and its neural circuits are depicted in Figure 2.

Relationship to Contrastive Hebbian Learning: When designing a network much as we do above, one might notice that the inference process is quite similar to that of a neural system learned under contrastive Hebbian learning (CHL) [28], although there are several significant differences. Layer activities in a CHL-based system are updated as follows:

$$\mathbf{z}^\ell(t) = \mathbf{z}^\ell(t-1) + \beta \left(-\mathbf{z}^\ell(t-1) + \phi^\ell(\mathbf{W}^\ell \cdot \mathbf{z}^{\ell-1}(t-1) + (\mathbf{W}^{\ell+1})^T \cdot \mathbf{z}^{\ell+1}(t-1)) \right) \quad (11)$$

where we notice that dynamics do not involve any normalization and the values for any layer ℓ are integrated a bit differently than in Equation 3, i.e., neural values change as a function of a form of a leaky Euler integration, where the top-down and bottom-up transmissions are combined to produce a perturbation to the layer rather than propose a new value of the state itself.

Like CHL, FF and PFF require two phases (or modes of computation) where the signals propagated through the neural system will be used in contrast with one another. Given data sample (\mathbf{x}, \mathbf{y}) , CHL specifically entails running the neural system first in an un-clamped phase (negative phase), where only the input image \mathbf{x} is clamped to the sensory input/bottom layer, followed by a clamped phase, where both \mathbf{x} and its target \mathbf{y} are clamped, i.e., \mathbf{y} is clamped to the output layer (positive phase). At the end of each phase (or inference cycle), the layer-wise activities are recorded and then used in a subtractive/contrastive Hebbian rule to calculate the updates for each matrix of

Algorithm 1 The predictive forward-forward (PFF) credit assignment algorithm. **red** denotes representation circuit computation and **blue** denotes generative circuit computation.

```

1: Input: sample  $(\mathbf{y}_i, \mathbf{x}_i)$ , data label  $c_i$  (binary label: 1 = "positive", 0 = "negative"), PFF parameters  $\Theta_r$  and  $\Theta_g$ 
2: Hyperparameters: State interpolation  $\beta$ , SGD step size  $\eta$ , noise scales  $\sigma_r$  and  $\sigma_z$ , stimulus time  $T$ 
3: // Note that  $\text{LN}(\mathbf{z}^\ell) = \mathbf{z}^\ell / (\|\mathbf{z}^\ell\|_2 + 1e-8)$ 
4: function SIMULATE $((\mathbf{y}_i, \mathbf{x}_i, c_i), \Theta_r, \Theta_g)$ 
5:   // Run forward pass to get initial activities
6:    $\mathbf{z}^0 = \mathbf{x}_i$ ,  $\mathbf{z}^\ell = \phi^\ell(\mathbf{W}^\ell \cdot \mathbf{z}^{\ell-1})$ , for  $\ell = 1, 2, \dots, L$ ,  $\mathbf{z}^{L+1} = \mathbf{y}_i$ ,  $\hat{\mathbf{z}}^{L+1} = \mathbf{0}$  (same as  $\mathbf{z}_s$ )
7:   for  $t = 1$  to  $T$  do
8:     // Run representation circuit
9:     for  $\ell = 1$  to  $L$  do ▷ Compute representation activities with layer-wise parameters  $\Theta_r^\ell = \{\mathbf{W}^\ell, \mathbf{V}^\ell\}$ 
10:       $\Theta_r^\ell = \Theta_r[\ell]$ ,  $\mathbf{W}^\ell, \mathbf{V}^\ell \leftarrow \Theta_r^\ell$  ▷ Extract relevant parameters
11:       $\epsilon_r^\ell \sim \mathcal{N}(0, \sigma_r)$ ,  $\mathbf{z}^\ell(t) = \beta(\phi^\ell(\mathbf{W}^\ell \cdot \text{LN}(\mathbf{z}^{\ell-1}(t-1)) + \mathbf{V}^\ell \cdot \text{LN}(\mathbf{z}^{\ell+1}(t-1))) + \epsilon_r^\ell) + (1-\beta)\mathbf{z}^\ell(t-1)$ 
12:      Calculate local goodness loss  $\mathcal{L}(\Theta_r^\ell)$  (Equation 1 using data label  $c_i$ )
13:       $\Delta \mathbf{W}^\ell = \left(2 \frac{\partial \mathcal{L}(\Theta_r^\ell)}{\partial \sum_j \epsilon_j^\ell (\mathbf{z}_j^\ell)^2} \odot \mathbf{z}^\ell\right) \cdot (\text{LN}(\mathbf{z}^{\ell-1}))^T$ ,  $\Delta \mathbf{V}^\ell = \left(2 \frac{\partial \mathcal{L}(\Theta_r^\ell)}{\partial \sum_j \epsilon_j^\ell (\mathbf{z}_j^\ell)^2} \odot \mathbf{z}^\ell\right) \cdot (\text{LN}(\mathbf{z}^{\ell+1}))^T$ 
14:       $\mathbf{W}^\ell \leftarrow \mathbf{W}^\ell - \eta \Delta \mathbf{W}^\ell$ ,  $\mathbf{V}^\ell \leftarrow \mathbf{V}^\ell - \eta \Delta \mathbf{V}^\ell$  ▷ SGD update with step size  $\eta$  shown (could use Adam [22] instead)
15:   // Run generative circuit
16:   for  $\ell = L$  to  $1$  do ▷ Compute generative predictions with layer-wise parameters  $\Theta_g^\ell = \{\mathbf{G}^\ell\}$ 
17:      $\Theta_g^\ell = \Theta_g[\ell]$ ,  $\mathbf{G}^\ell \leftarrow \Theta_g^\ell$  ▷ Extract relevant parameters
18:      $\epsilon_g^\ell \sim \mathcal{N}(0, \sigma_z)$ ,  $\hat{\mathbf{z}}^{\ell+1} = \phi^{\ell+1}(\mathbf{z}^{\ell+1} + \epsilon_g^{\ell+1})$ ,  $\bar{\mathbf{z}}^\ell = \phi^\ell(\mathbf{G}^\ell \cdot \text{LN}(\hat{\mathbf{z}}^{\ell+1}))$ 
19:     Calculate local generative loss  $\mathcal{L}_g^\ell(\mathbf{G}^\ell) = \frac{1}{2} \sum_j (\bar{\mathbf{z}}_j^\ell - \mathbf{z}_j^\ell(t))^2$ 
20:      $\mathbf{e}^\ell = \bar{\mathbf{z}}^\ell - \mathbf{z}^\ell$ ,  $\Delta \mathbf{G}^\ell = \mathbf{e}^\ell \cdot (\text{LN}(\mathbf{z}^{\ell+1}(t)))^T$  ▷ Note that  $\mathbf{e}^\ell = \frac{\partial \mathcal{L}_g^\ell(\mathbf{G}^\ell)}{\partial \bar{\mathbf{z}}^\ell}$ 
21:      $\mathbf{G}^\ell \leftarrow \mathbf{G}^\ell - \eta \Delta \mathbf{G}^\ell$ 
22:      $\mathbf{z}^{L+1} \leftarrow \mathbf{z}^{L+1} - \gamma \frac{\partial \mathcal{L}_g^L(\mathbf{G}^L)}{\partial \mathbf{z}^{L+1}}$  ▷ Update latent variable  $\mathbf{z}_s$  (one step of iterative inference)
23: Return  $\Theta_g, \Theta_r$  ▷ Output newly updated PFF parameters

```

synapses. Note that the positive phase of CHL depends on first running the negative phase. FF and PFF, in contrast, essentially amount to running the positive and negative phases in parallel (with each phase conditioned on different data), resulting in an overall faster pattern processing time (instead of one inference cycle being conditioned on the statistics of another, the same cycles are now run on either positive or negative data with opposite objectives [16]).

Relationship to Predictive Coding: The PFF algorithm integrates the local hypothesis generation component of predictive coding (PC) into the inference process by leveraging the representations acquired within the recurrent representation network’s iterative processing window. Specifically, each layer of the representation circuit, at each time step, becomes the prediction target for each layer of the generative circuit. In contrast, PC generative models must leverage a set of feedback synapses to progressively modify their layerwise neural activities before finally adjusting synaptic values. Furthermore, PFF iteratively/dynamically modifies the synapses within each processing time step, whereas; typically, most PC circuits implement a form of expectation-maximization that, as a result, generally requires longer stimulus processing windows in order to learn effective generative models [32] given that Euler integration is being simulated (in this work, the PFF generative circuit learns a good-quality generative model in only 8 steps whereas the models of [32] required at least 50 steps).

Relationship to Local Learning: It has been strongly argued that the synapses in the brain are likely to be adjusted according to a local scheme, i.e., only information closest spatially and in time to a target synapse is involved in computing its change in efficacy. Methods that adhere to this biological constraint/setup are referred to as local learning procedures [35, 25, 29, 30, 4, 21], offering a potential replacement for backprop for training deep neural networks, relaxing one or more of its core constraints (see Figure 3 for details related to some of the key ones). Desirably, it has even been shown that, empirically, updates from a local scheme can result in improved model generalization [25, 35]. There have been many efforts in designing biologically-plausible local learning algorithms, such as contrastive Hebbian learning (mentioned above) [28], contrastive divergence for learning harmoniums (or restricted Boltzmann machines) [17], the wake-sleep algorithm for learning Helmholtz machines [18], and algorithms such as equilibrium propagation [43]. Other efforts that directly integrate local learning into the deep learning pipeline include kickback [1] and decoupled neural interfaces [20]. It is worth pointing out that PFF does bear some similarity to the wake-sleep algorithm, which itself entails learning a generative model jointly with an inference (recognition) model. However, the wake-sleep algorithm suffers from instability, given that the recognition network could be damaged by random fantasies produced by the generative network and the generative network could itself be hampered by the low-quality representation capability of the inference network (motivating

Learning Algorithms	BP	FA	PC	LRA	NGC	FF	PFF
Fwd locked	<i>Global</i>	<i>Global</i>	<i>Local</i>	<i>Local</i>	<i>Local</i>	<i>None</i>	<i>None</i>
Fwd error							
Fwd target							
Bwd locked	<i>Global</i>	<i>Global</i>	<i>None</i>	<i>None</i>	<i>None</i>	<i>None</i>	<i>None</i>
Bwd error							
Bwd target							
Local loss							
Error Synapses		<i>Fixed</i>		<i>Learned</i>	<i>Learned</i>		
Global signal							
Local Signal							
Generative capabilities							
Generative Weights							

Figure 3: Properties of different learning algorithms, i.e., backprop (BP), feedback alignment (FA), predictive coding (PC), local representation alignment (LRA), neural generative coding (NGC), the forward-forward algorithm (FF), and the predictive forward-forward process (PFF).

the design of improvements, such as reweighted wake-sleep [6]). PFF, in contrast, aims to learn the generative model given the representation circuit, using the locally-adapted distributed neural activities as a guide for the synthesization process rather than randomly sampling the generative model to generate teaching signals for the recognition network (potentially distracting its optimization with nonsensical noisy signals).

3 Experiments

This section describes the simulations/experiments that were run to test the proposed PFF procedure. We leverage several benchmark image datasets to quantitatively evaluate PFF’s classification ability (in terms of test-set error) and qualitatively evaluate its generative capability (in terms of visual inspection of sample reconstruction and pattern synthesization). The PFF process (PFF-RNN) is compared with the FF algorithm (FF) as well as several baselines, including the K -nearest neighbors algorithm (with $K = 4$, or 4-KNN), the recurrent network trained with the original FF algorithm [16], and two backprop-based models, i.e., a feedforward network that uses backprop to adjust all of its internal synapses (BP-FNN) and the same network but one that only adjusts the top-most softmax/output layer parameters and fixes the hidden layer synaptic parameters (Rnd-FNN). Both backprop-based networks are trained to minimize the categorical cross-entropy of each dataset’s provided labels. The partially-trained model, i.e., the Rnd-FNN, serves as a sort of lower bound on the generalization ability of a neural system, given that it is possible to obtain respectable classification performance with only random hidden feature detectors (a neural credit assignment algorithm should not perform worse than this).

Datasets: In this study, we experiment with two (gray-scale) image collections, i.e., the MNIST and the Kuzushiji-MNIST databases. The MNIST dataset [24] specifically contains 28×28 images containing handwritten digits across 10 different categories. Kuzushiji-MNIST (KMIST) is a challenging drop-in replacement for MNIST, containing 28×28 images depicting hand-drawn Japanese Kanji characters [7] (each class corresponding to the character’s modern hiragana counterpart, with 10 classes in total).

Table 1: Classification generalization results for neural systems trained under different learning algorithms (except for 4-KNN, which is a non-parametric learning baseline model). Measurements of mean and standard deviation are made across five experimental trial runs.

Model	MNIST	K-MNIST
	Test Error (%)	Test Error (%)
4-KNN	2.860 ± 0.000	7.900 ± 0.000
Rnd-FNN	3.070 ± 0.018	14.070 ± 0.189
BP-FNN	1.300 ± 0.023	6.340 ± 0.202
FF-RNN [16]	1.320 ± 0.100	6.590 ± 0.420
PFF-RNN	1.360 ± 0.030	6.460 ± 0.120

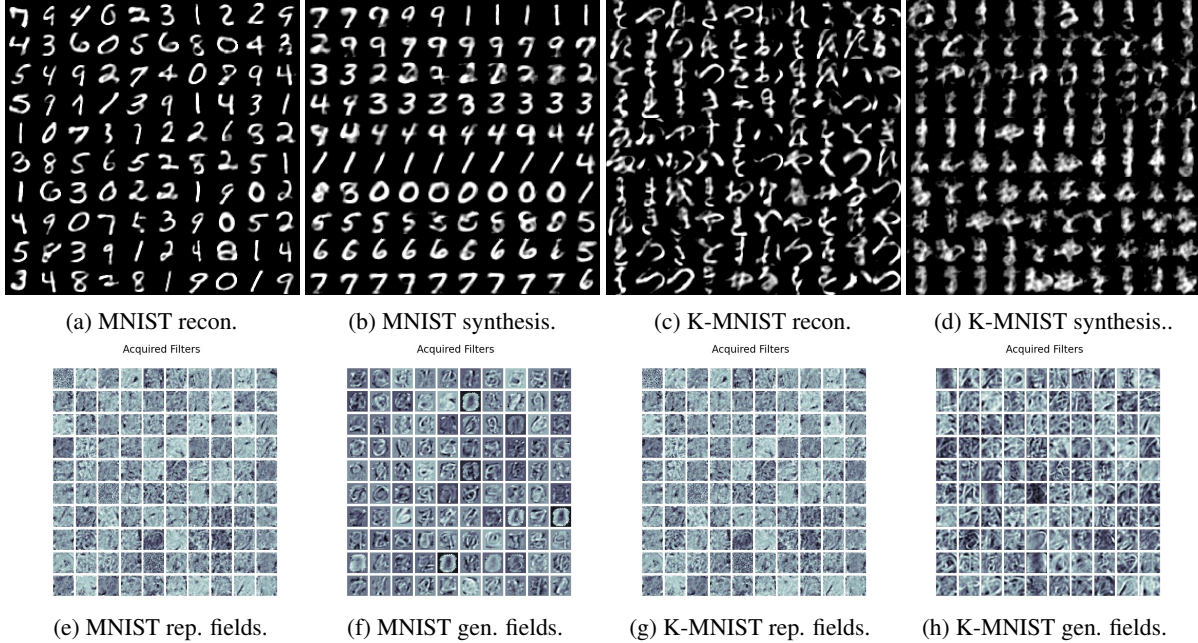


Figure 4: Model reconstruction (Left) and generated (Right) samples for MNIST and K-MNIST. In the bottom row, the receptive fields of the bottom-most layer of the representation (rep.) circuit (Left) and those of the generative (gen.) circuit (Right) are displayed.

Simulation Setup: All models simulated in this study were constrained to use similar architectures in order to ensure a more fair comparison. All networks for all neural-based learning algorithms contained two hidden layers of 2000 neurons (which was also done for the FF models in [16]), with initial synaptic weight values selected according to the random orthogonal initialization scheme [42] (using singular value decomposition). Once any given learning algorithm calculated adjustment values for the synapses, parameters were adjusted, using the Adam adaptive learning rate [22] with mini-batches containing 500 samples. Both FF and PFF were set to use a threshold value of $\theta_z = 10.0$ and PFF was set to use 20 latent variables (i.e., $\mathbf{z}_s \in \mathcal{R}^{20 \times 1}$), representation noise $\epsilon^\ell = 0.05$, and generative noise $\epsilon_z = 0.025$.

3.1 Discussion

Observe in Table 1 that the PFF procedure performs well in the context of the models simulated in this study, reaching a top/good-quality classification error of about 1.36% on MNIST, nearly reaching that of the well-tuned backprop-based classifier BP-FNN. Notably, the PFF-RNN model outperforms BP-FNN slightly on K-MNIST, arguably a more difficult benchmark. Both FF and PFF outperform the lower-bound baselines, i.e., 4-KNN and Rnd-FNN, indicating that they acquire hidden feature detectors that facilitate good discriminative performance.

Qualitatively, in Figure 4 (Top Row), observe that PFF learns a good-quality reconstruction model and generative model of the image inputs. The reconstructed digits and Kanji characters are excellent and the image samples for both cases exhibit variety/diversity across the categories (albeit a bit blurry). Note that to sample from the PFF’s directed generative model, as mentioned earlier in Section 2.3, we retro-fit a GMM to samples of its latent

variable \mathbf{z}_s , specifically optimizing a GMM via expectation-maximization with 10 components. In addition, as shown in the bottom row of Figure 4, the receptive fields (of the synapses of the layer closest to the sensory input layer) acquired by the fully-connected representation circuits of both the representation and generative circuits appear to extract useful/interesting structure related to digit or Kanji character strokes, often, as is expected for fully-connected neural structures, acquiring representative full object templates (if one desired each receptive field to acquire only single strokes/component features specifically, then an additional prior would need to be imposed, such as convolution or the locally-connected receptive field structure employed in [2, 16]).

4 Conclusion

In this work, we proposed the predictive forward-forward (PFF) process for dynamically adjusting the synaptic efficacies of a recurrent neural system that jointly learns how to classify, reconstruct, and synthesize data samples without backpropagation of errors. Our model and credit assignment procedure integrates elements of the forward-forward algorithm, such as its local synaptic adaptation rule based on goodness and contrastive learning, with aspects of predictive coding, such as its local error Hebbian manner of adjusting generative synaptic weights, resulting in a promising brain-inspired, forward-only and backprop-free form of machine learning.

References

- [1] BALDUZZI, D., VANCHINATHAN, H., AND BUHMANN, J. M. Kickback cuts backprop’s red-tape: Biologically plausible credit assignment in neural networks. In *AAAI* (2015), pp. 485–491.
- [2] BARTUNOV, S., SANTORO, A., RICHARDS, B., MARRIS, L., HINTON, G. E., AND LILLICRAP, T. Assessing the scalability of biologically-motivated deep learning algorithms and architectures. In *Advances in Neural Information Processing Systems* (2018), pp. 9390–9400.
- [3] BASTOS, A. M., USREY, W. M., ADAMS, R. A., MANGUN, G. R., FRIES, P., AND FRISTON, K. J. Canonical microcircuits for predictive coding. *Neuron* 76, 4 (2012), 695–711.
- [4] BELILOVSKY, E., EICKENBERG, M., AND OYALLON, E. Decoupled greedy learning of cnns. In *International Conference on Machine Learning* (2020), PMLR, pp. 736–745.
- [5] BENGIO, Y., LAUFER, E., ALAIN, G., AND YOSINSKI, J. Deep generative stochastic networks trainable by backprop. In *International Conference on Machine Learning* (2014), PMLR, pp. 226–234.
- [6] BORNSCHEIN, J., AND BENGIO, Y. Reweighted wake-sleep. *arXiv preprint arXiv:1406.2751* (2014).
- [7] CLANUWAT, T., BOBER-IRIZAR, M., KITAMOTO, A., LAMB, A., YAMAMOTO, K., AND HA, D. Deep learning for classical japanese literature, 2018.
- [8] CRICK, F. The recent excitement about neural networks. *Nature* 337, 6203 (1989), 129–132.
- [9] FLORIDI, L., AND CHIRIATTI, M. Gpt-3: Its nature, scope, limits, and consequences. *Minds and Machines* 30, 4 (2020), 681–694.
- [10] FRISTON, K. The free-energy principle: a unified brain theory? *Nature reviews neuroscience* 11, 2 (2010), 127–138.
- [11] GOLDMAN, M. S. Memory without feedback in a neural network. *Neuron* 61, 4 (2009), 621–634.
- [12] GROSSBERG, S. Competitive learning: From interactive activation to adaptive resonance. *Cognitive science* 11, 1 (1987), 23–63.
- [13] GUTMANN, M., AND HYVÄRINEN, A. Noise-contrastive estimation: A new estimation principle for unnormalized statistical models. In *Proceedings of the thirteenth international conference on artificial intelligence and statistics* (2010), JMLR Workshop and Conference Proceedings, pp. 297–304.
- [14] HEBB, D. O., ET AL. The organization of behavior, 1949.
- [15] HELMHOLTZ, H. v. Treatise on physiological optics, 3 vols.
- [16] HINTON, G. The forward-forward algorithm: Some preliminary investigations. <https://www.cs.toronto.edu/hinton/FFA13.pdf> (2022).
- [17] HINTON, G. E. Training products of experts by minimizing contrastive divergence. *Neural computation* 14, 8 (2002), 1771–1800.
- [18] HINTON, G. E., DAYAN, P., FREY, B. J., AND NEAL, R. M. The "wake-sleep" algorithm for unsupervised neural networks. *Science* 268, 5214 (1995), 1158–1161.

- [19] HINTON, G. E., AND MCCLELLAND, J. L. Learning representations by recirculation. In *Neural information processing systems* (1988), pp. 358–366.
- [20] JADERBERG, M., CZARNECKI, W. M., OSINDERO, S., VINYALS, O., GRAVES, A., AND KAVUKCUOGLU, K. Decoupled neural interfaces using synthetic gradients. *arXiv preprint arXiv:1608.05343* (2016).
- [21] KAISER, J., MOSTAFA, H., AND NEFTCI, E. Synaptic plasticity dynamics for deep continuous local learning (decolle). *Frontiers in Neuroscience* 14 (2020), 424.
- [22] KINGMA, D., AND BA, J. Adam: A method for stochastic optimization. *arXiv preprint arXiv:1412.6980* (2014).
- [23] LAROCHELLE, H., AND BENGIO, Y. Classification using discriminative restricted boltzmann machines. In *Proceedings of the 25th international conference on Machine learning* (2008), pp. 536–543.
- [24] LECUN, Y. The mnist database of handwritten digits. <http://yann.lecun.com/exdb/mnist/> (1998).
- [25] LEE, D.-H., ZHANG, S., FISCHER, A., AND BENGIO, Y. Difference target propagation. In *Joint European Conference on Machine Learning and Knowledge Discovery in Databases* (2015), Springer, pp. 498–515.
- [26] LILLICRAP, T. P., COWNDEN, D., TWEED, D. B., AND AKERMAN, C. J. Random feedback weights support learning in deep neural networks. *arXiv preprint arXiv:1411.0247* (2014).
- [27] MARBLESTONE, A. H., WAYNE, G., AND KORDING, K. P. Toward an integration of deep learning and neuroscience. *Frontiers in computational neuroscience* (2016), 94.
- [28] MOVELLAN, J. R. Contrastive hebbian learning in the continuous hopfield model. In *Connectionist models*. Elsevier, 1991, pp. 10–17.
- [29] NØKLAND, A. Direct feedback alignment provides learning in deep neural networks. In *Advances in Neural Information Processing Systems* (2016), pp. 1037–1045.
- [30] NØKLAND, A., AND EIDNES, L. H. Training neural networks with local error signals. In *Proceedings of the 36th International Conference on Machine Learning* (09–15 Jun 2019), K. Chaudhuri and R. Salakhutdinov, Eds., vol. 97 of *Proceedings of Machine Learning Research*, PMLR, pp. 4839–4850.
- [31] OLSHAUSEN, B. A., AND FIELD, D. J. Sparse coding with an overcomplete basis set: A strategy employed by v1? *Vision research* 37, 23 (1997), 3311–3325.
- [32] ORORBIA, A., AND KIFER, D. The neural coding framework for learning generative models. *Nature communications* 13, 1 (2022), 1–14.
- [33] ORORBIA, A., MALI, A., GILES, C. L., AND KIFER, D. Continual learning of recurrent neural architectures by locally aligning distributed representations. *arXiv preprint arXiv:1810.07411* (2018).
- [34] ORORBIA, A., MALI, A., KIFER, D., AND GILES, C. L. Lifelong neural predictive coding: Sparsity yields less forgetting when learning cumulatively. *arXiv preprint arXiv:1905.10696* (2019).
- [35] ORORBIA, A. G., AND MALI, A. Biologically motivated algorithms for propagating local target representations. In *Proceedings of the AAAI Conference on Artificial Intelligence* (2019), vol. 33, pp. 4651–4658.
- [36] ORORBIA, A. G., REITTER, D., WU, J., AND GILES, C. L. Online learning of deep hybrid architectures for semi-supervised categorization. In *Joint European Conference on Machine Learning and Knowledge Discovery in Databases* (2015), Springer, pp. 516–532.
- [37] RAO, R. P., AND BALLARD, D. H. Predictive coding in the visual cortex: a functional interpretation of some extra-classical receptive-field effects. *Nature neuroscience* 2, 1 (1999).
- [38] RUMELHART, D. E., HINTON, G. E., AND WILLIAMS, R. J. Learning representations by back-propagating errors. *nature* 323, 6088 (1986), 533–536.
- [39] SALAKHUTDINOV, R., AND LAROCHELLE, H. Efficient learning of deep boltzmann machines. In *Proceedings of the thirteenth international conference on artificial intelligence and statistics* (2010), JMLR Workshop and Conference Proceedings, pp. 693–700.
- [40] SALVATORI, T., SONG, Y., HONG, Y., SHA, L., FRIEDER, S., XU, Z., BOGACZ, R., AND LUKASIEWICZ, T. Associative memories via predictive coding. *Advances in Neural Information Processing Systems* 34 (2021), 3874–3886.
- [41] SALVATORI, T., SONG, Y., XU, Z., LUKASIEWICZ, T., BOGACZ, R., LIN, H., FAN, Y., ZHANG, J., BAI, B., XU, Z., ET AL. Reverse differentiation via predictive coding. In *Proceedings of the 36th AAAI Conference on Artificial Intelligence , AAAI 2022 , Vancouver, BC, Canada, February 22–March 1 , 2022* (2022), vol. 10177, AAAI Press, pp. 507–524.

- [42] SAXE, A. M., MCCLELLAND, J. L., AND GANGULI, S. Exact solutions to the nonlinear dynamics of learning in deep linear neural networks. *arXiv preprint arXiv:1312.6120* (2013).
- [43] SCELLIER, B., AND BENGIO, Y. Equilibrium propagation: Bridging the gap between energy-based models and backpropagation. *Frontiers in computational neuroscience* 11 (2017), 24.
- [44] SILVER, D., HUANG, A., MADDISON, C. J., GUEZ, A., SIFRE, L., VAN DEN DRIESSCHE, G., SCHRIETWIESER, J., ANTONOGLOU, I., PANNEERSHELVAM, V., LANCTOT, M., ET AL. Mastering the game of go with deep neural networks and tree search. *nature* 529, 7587 (2016), 484–489.

Appendix

Visualized Samples (Expanded)

This appendix section presents the reconstruction and synthesized samples from the PFF models in the main paper at a larger image scale/size.



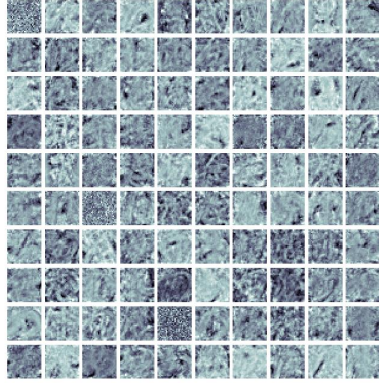
(a) PFF reconstructed images.



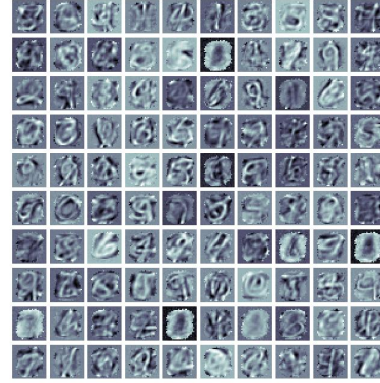
(b) PFF sampled images.

Acquired Filters

Acquired Filters

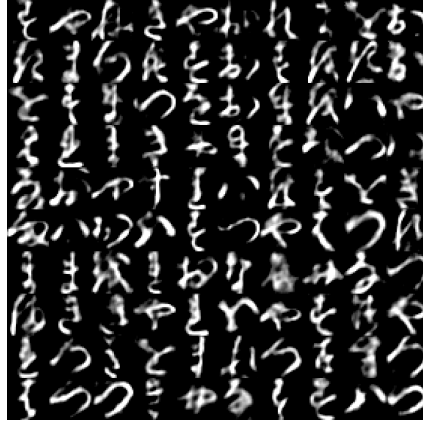


(c) PFF representation receptive fields.

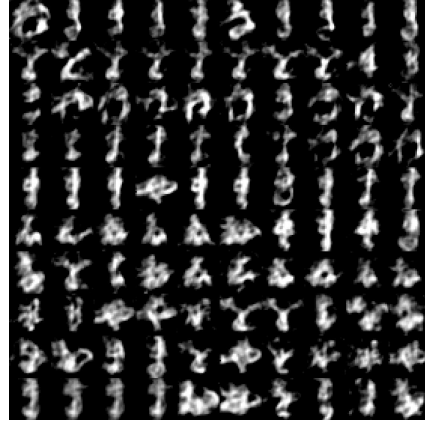


(d) PFF generative receptive fields.

Figure 5: MNIST model reconstruction (Left) and generated (Right) samples. In the bottom row, the receptive fields of the bottom-most layer of the representation circuit (Left) and those of the generative circuit (Right).



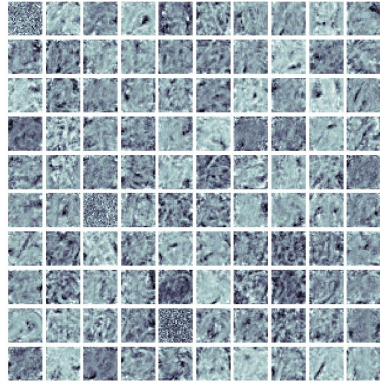
(a) PFF reconstructed images.



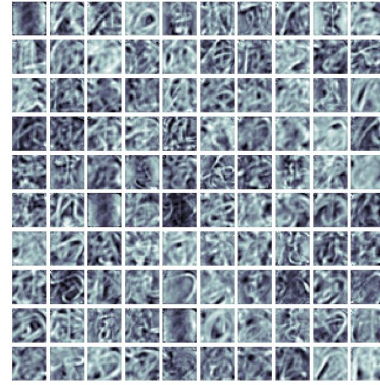
(b) PFF sampled images.

Acquired Filters

Acquired Filters



(c) PFF representation receptive fields.



(d) PFF generative receptive fields.

Figure 6: In the top row, Kuzushiji-MNIST model reconstruction (Left) and generated (Right) samples. In the bottom row, the receptive fields of the bottom-most layer of the representation circuit (Left) and those of the generative circuit (Right).